Performance Analysis of a Rotating Circular Array for Plane Wave Identification

Frederico Araujo[1,2], Fernando Pinto[2], Michael Vorländer[1]

[1] *Institut für Technische Akustik, RWTH Aachen University, 52074 Aachen,*
E-Mail:[frederico.araujo, mvo]@akustik.rwth-aachen.de
[2] *Laboratório de Acústica e Vibrações, UFRJ, 21941-914 Rio de Janeiro,*
E-Mail: [fh.araujo, fcpinto]@ufrj.br

Introduction

One advantage of a Spherical Microphone Array (SMA) is the possibility to analyze all directions in space with similar efficiency, but it usually requires a high number of microphones, each one associated with a measurement point, to be able to have a good spatial resolution. This requirement usually means an increase in the array cost.

This paper shows the development of a rotating circular array with 14 microphones, resulting in a virtual SMA with 98 measurement points. Aiming the identification of direction and time of arrival of plane waves in a reverberant field, this array geometry allows a spherical harmonic expansion up to 6th order.

It is presented the comparison between simulations and measurements with the proposed array, using the Spherical Harmonic Beamforming.

Spherical Harmonic Beamforming

The spherical harmonics are an orthonormal base of functions that are obtained by solving the wave equation for spherical coordinates. The degree n and order m spherical harmonic is given by:

$$Y_n^m(\theta,\phi) = \sqrt{\frac{2n+1}{4\pi}\frac{n-m}{n+m}}P_n^m(\cos\theta)e^{im\phi} \tag{1}$$

where θ and φ are the elevation and azimuth angles, respectively, and P_n^m is the associated Legendre polynomial. Considering a function $f(\theta,\varphi)$ which is entirely defined and integrable on the surface, Ω, of a unit sphere, it is possible to decompose it in spherical harmonics in the following way:

$$f(\theta,\varphi) = \sum_{n=0}^{\infty}\sum_{m=-n}^{n}\overline{f_{nm}}\ Y_n^m(\theta,\varphi) \tag{2}$$

The overline f is the degree n and order m coefficient, it can be obtained by:

$$\overline{f_{nm}} = \int_{\Omega} f(\theta,\varphi)Y_n^m(\theta,\varphi)^* d\Omega \tag{3}$$

where * is the conjugated complex representation.

The advantage of the spherical arrays is the possibility of having the same beampattern for all the directions in space. The ideal beampattern is a Dirac delta in this application, where the direction of interest has unitary gain and all the others have none. The generic spherical harmonic beamforming expression for a driven direction (θ_s,φ_s) is given by:

$$B(ka,\theta_s,\varphi_s) = \int_{\Omega} w(ka,\theta,\varphi,\theta_s,\varphi_s)P(\omega,\theta,\varphi)d\Omega \tag{4}$$

where w is the steering vector that drive the algorithm for the direction (θ_s,φ_s), k is the wave number, a is the sphere radius and P is the Fourier Transform of the pressure over the sphere surface.

Using the spherical harmonic decomposition, the ideal beampattern can be expressed by the spherical harmonics:

$$\delta(\theta-\theta_s)\delta(\varphi-\varphi_s) = \sum_{n=0}^{\infty}\sum_{m=-n}^{n}\overline{\delta_{nm}}Y_n^m(\theta,\varphi) \tag{5}$$

where

$$\overline{\delta_{nm}} = Y_n^m(\theta_s,\varphi_s) \tag{6}$$

Therefore, the ponderation, assuming that the sound field is composed only by plane waves, is given by [1]

$$w = \sum_{n=0}^{\infty}\sum_{-n}^{n}\frac{\overline{\delta_{nm}}}{4\pi i b_n(ka)}Y_n^m(\theta,\varphi) \tag{7}$$

where b_n is the mode strength and it is given by:

$$b_n(ka) = j_n(ka) \tag{8}$$

for open spheres (where the spherical surface is virtual) and

$$b_n(ka) = j_n(ka) - \frac{j'_n(ka)}{h'_n(ka)}h_n(ka) \tag{9}$$

for rigid spheres. Where j_n and h_n is the Bessel spherical function and Henkel spherical function, respectively, j'_n and h'_n are their derivatives. The second term in the right side in Eq. [9] is due the scattering around the rigid surface.

The mode strength can be seen in Figure 1, for the rigid and open sphere cases. It can be noticed that some amplitudes become null or very small for specific ka values for the open sphere. The advantage of the rigid sphere, over the open one, is its numerical stability, due to the inversion of b_n, as seen in Equation (7). For the open sphere, the mode strength approaching zero for certain frequencies might lead to numerical instability and uncertainties. The advantage of the last one would be the ease in the fabrication when compared

with the rigid one with the same measuring points distribution.

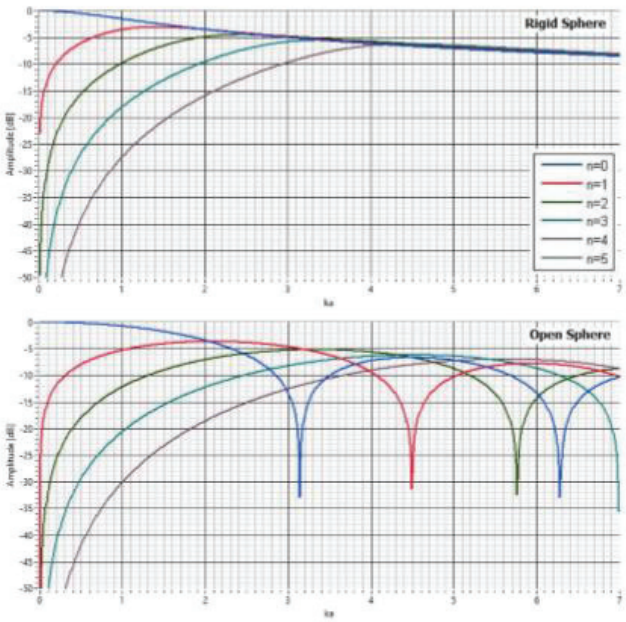

Figure 1: Mode strength, $b_n(ka)$, for rigid (top) and open (bottom) spheres, for order n = 0 to 5.

In practice, the pressure is not known along the entire sphere surface, only in discrete points where the microphones are positioned. For this reason, the beamforming integration becomes a summation:

$$\sum_{j=1}^{M} \alpha_j w(ka, \theta_s, \varphi_s, \theta, \varphi) P(ka, \theta, \varphi) \tag{10}$$

where α_j is the term responsible to compensate the distribution of the sample points and make the summation converge.

Consequently, it will not be possible to expand the ideal beampattern to infinity orders. Generally, to ensure a truncation of the harmonic spherical decomposition in order N, it is necessary M microphones [2], where:

$$M \geq (N+1)^2 \tag{11}$$

For greater N, the beampattern will be closer from the Dirac delta. The Figure 2 shows beampattern truncated for different N values.

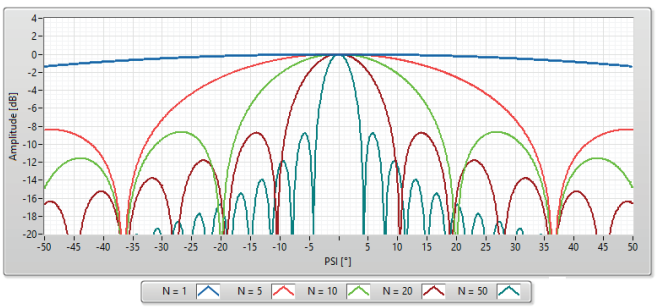

Figure 2: Beampattern truncated in order N = 1, 5, 10, 20 and 50

Therefore, the spatial resolution Ψ_0 will become tighter the greater N, that means, the greater is the number or measuring points:

$$2\Psi_0 \approx \frac{2\pi}{N} \approx \frac{2\pi}{\sqrt{M}} \tag{12}$$

Microphone Array

As shown in the previous section, to achieve better spatial resolution it is necessary to increase the number of measuring points. But the measuring points usually is limited by the number of sensor and input channels in the acquisition boards available. That means, to improve the spatial resolution, in general cases, it leads to an increase in the cost of the array.

For these reasons, it is proposed a rotating microphone array (Figure 3) consisting in 14 microphones distributed in a circle with radius 100 mm, according with the Gaussian sampling [1]. Sampling the sound field in 7 different angles, around the central metal shaft, it is formed a virtual spherical array, an open sphere with 98 measuring points. The rotation is made by a control system using a potentiometer and a step motor.

This number allows the expansion in spherical harmonics up to order $N = 6$. The frequency range expect for this array is between the 1250 and 2500 third octave [3].

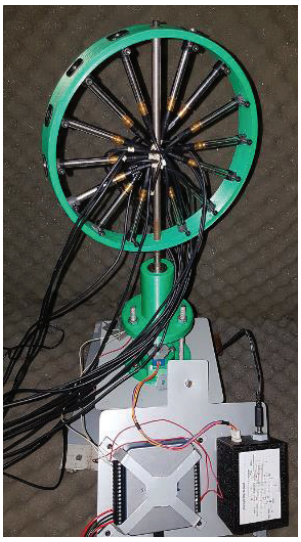

Figure 3: Rotating microphone array

Figure 4 shows the three main error sources for the spherical harmonic beamforming for the open sphere [4]. The error in positioning the microphones and the error due to the transducer noise have the same behavior. Both have significantly greater error for lower frequencies and slightly increasing error for higher frequencies, having a minimum value at $ka = N$, adding some peaks due to the division by b_n., that tends to zero for some arguments, as seen in Figure 1.

For the spherical harmonics aliasing, the error is small for lower frequencies and increases for higher frequencies. These errors will determinate the real frequency range of the array.

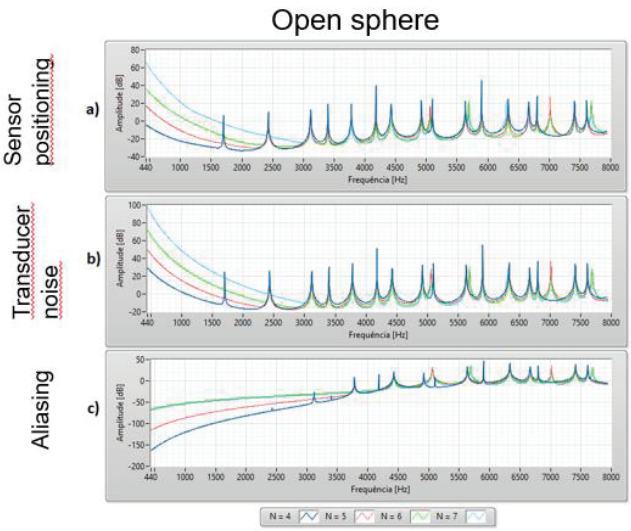

Figure 4: Errors in the spherical harmonic beamforming over the frequency

Simulations

Using the geometry of this 98-points spherical microphone array, two situations were simulated:

- Stationary sound source emitting a white noise arriving at the spherical array in the direction $(\theta_0, \varphi_0) = (90°, 180°)$. A time window of 0.1 s was used.
- Sound source emitting broadband impulse arriving at $(\theta_0, \varphi_0) = (90°, 180°)$, with the experimental procedure shown in Figure 5. In this case, the maps were made for the exactly instant of arrival of the impulse.

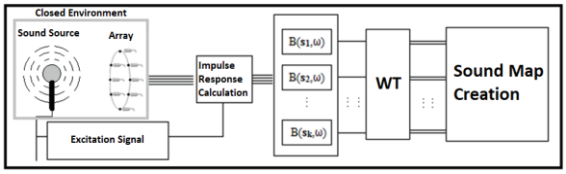

Figure 5: Procedure adopted for the creation of the impulse response maps [5]

Figure 6 and 7 show the results for each case, respectively.

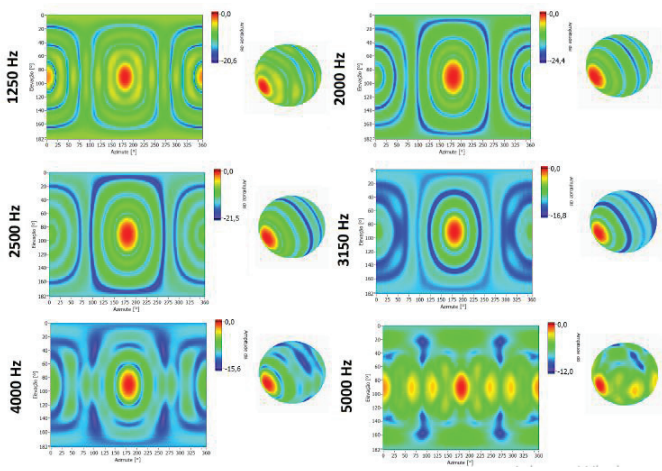

Figure 6: Sound maps of the simulation for stationary sound source emitting a white noise

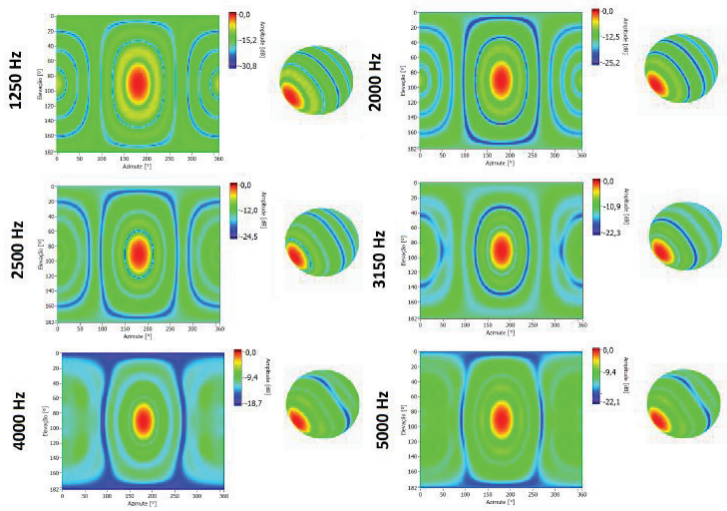

Figure 7: Sound maps of the simulation for the instant of arrival of the broadband impulse

For the boths cases, it can be seen that the simulations confirms the expect frequency range. Above 2500 Hz, it is observed some distortions in the main lobe that can be explained by the truncation in the spherical harmonic decomposition in order $N = 6$.

Measurements

The same two previous situations were measured using a mini chamber with approximately 0.4 m³ and with all surfaces covered with an acoustic foam. For this configuration, the mini chamber has a reverberation time (T_{20}) of 0.015 s. Figure 9 and 10 show the results for each case, respectively. In these measurements, the direction (θ_0, φ_0) of the sound source was shifted to appear in the center of the map.

Figure 8: Mini chamber, covered with acoustic foam, used in the measurements

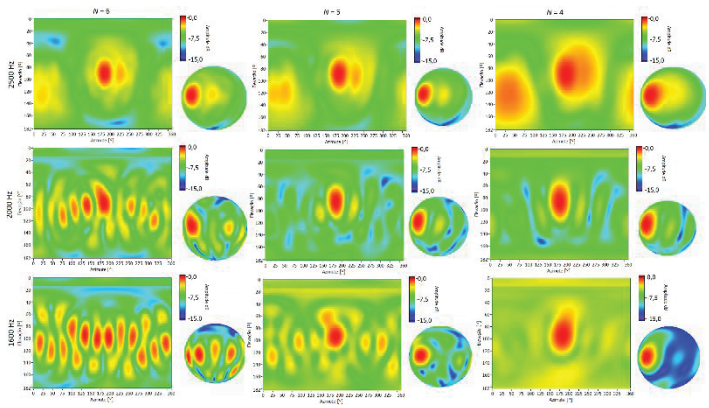

Figure 9: Sound maps of the measurement for stationary sound source emitting a white noise

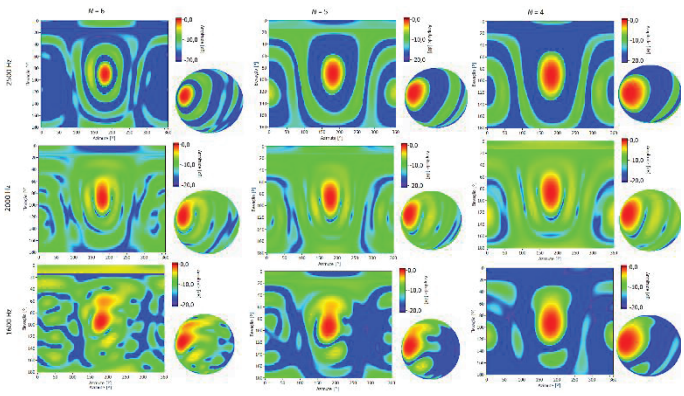

Figure 10: Sound maps of the measurment for the instant of arrival of the broadband impulse

It can be seen that, in both cases, the results differ from the simulation, especially for higher *N* and lower frequency. This can be explained by the error in the sensor positioning, as shown in Fig. 4a. In Fig. 9, it also can be seen some concentration of energy that does not correspond to the direction of the direct sound. This is because of the acoustic foams that do not absorb all the sound energy, for this reason, it will still be there first order reflections in the sound maps.

Conclusion

It was designed and built a rotating microphone array with 98 virtual measuring points distributed in a spherical surface of radius 100 mm. The main objective was to calculate the directional impulse response for late reverberation reflections identification, using a low-cost spherical array that allowed a properly spatial resolution for this application.

The simulations showed that the desired spatial resolution can be achieved with the geometry proposed for the frequency range between the third octaves of 1250 and 2500 Hz, using spherical harmonics up to order $N = 6$. On the other hand, the measurement did not show this efficiency, presenting higher errors, especially, for lower frequency and for higher *N*. Before this array is used in room acoustics applications, as the one proposed in this paper, the error sources must be found and corrected.

One of the hypotheses that would explain this difference is the positioning error of the sensors. Since it is been analyzed a rotating array, this accuracy is harder to ensure, because the precision of the control system will never be perfect.

Another point that must be revised is the used of the mini chamber for the measurement, since it does not provide an anechoic environment, that means, unexpected reflections will appear in sound maps, mainly in the 1st situation with the sound source emitting a white noise.

Lastly, the open-sphere model should be also be revised. In this model, it is considered that the microphone array does not interfere in the sound field, but this assumption shall not be taken for higher frequency range.

Acknowledgement

Frederico Araujo would like to acknowledge the support from the Deutscher Akademischer Austauschdienst (DAAD), from the Laboratório de Acústica e Vibrações (LAVI/UFRJ) and the Institute of Technical Acoustics (ITA/RWTH Aachen University)

Reference

[1] Rafaely, B. "Analysis and design of spherical microphone arrays." IEEE Transactions on speech and audio processing 13.1: 135-143, 2005

[2] Meyer, J., Elko, G., “A highly scalable spherical microphone array based on an orthonormal decomposition of the sound field". In: Acoustics, Speech, and Signal Processing (ICASSP), 2002 IEEE International Conference on, v. 2, pp. II-1781. IEEE., 2002

[3] Abhayapala, T. D., Ward, D. B., 2002, “Theory and design of high order sound field microphones using spherical microphone array”. In: Acoustics, Speech, and Signal Processing (ICASSP), 2002 IEEE International Conference on, v. 2, pp. II–1949. IEEE

[4] Rafaely, B., Weiss, B., Bachmat, E., 2007, “Spatial aliasing in spherical microphone arrays”, IEEE Transactions on Signal Processing, v. 55, n. 3, pp. 1003–1010

[5] De Araujo, F. H., Pinto, F. A. D. N. C., Torres, J. C. B., 2018, “Room reflections analysis with the use of spherical beamforming and wavelets", Applied Acoustics, v. 131, pp. 192-202.